Optical Simulation of a Ring-Defect Photonic Crystal Vertical-Cavity Surface-Emitting Laser

Péter Nyakas
Furukawa Electric Institute of Technology, Ltd.
H-1158, Vasgolyó u. 2-4., Budapest, Hungary
Email: pnyakas@wigner.bme.hu

***Abstract*—A fully numerical solution of the scalar Helmholtz equation is applied for the optical mode calculation of a ring-defect photonic crystal vertical-cavity surface-emitting laser. It is shown that the diameter of the central hole determines which mode starts lasing at the threshold current. This confirms the result of a previous experimental work.**

I. Introduction

Vertical-cavity surface-emitting lasers (VCSELs) are promising devices on the semiconductor laser market due to their advantageous characteristics such as low threshold current, single-longitudinal mode operation, high modulation bandwidth, low cost and circular output-beam profile enabling efficient fiber coupling. Photonic crystal (PC) patterns etched into the top distributed Bragg reflector (DBR) of a VCSEL can be employed to produce single-mode lasers [1], although they do not provide the necessary current confinement. The efficient design of single-mode PC-VCSELs requires an analysis that incorporates the effects on both the refractive index profile and the optical loss obtained from the PC.

A large two-dimensional (2-D) array of VCSELs can constitute a broad area, high-power source with a narrow line width. Evanescent coupling between neighboring VCSELs can lock them together to operate in a single mode [2]. 2-D array configurations of PC-VCSELs were also investigated in the context of mode control. It was shown experimentally [3], [4] and theoretically [5] that it depended on the diameter of holes in both 2×1 and 2×2 arrays whether in-phase or out-of-phase coupling between adjacent defects was preferred.

An oxide-confined ring-defect (RD) PC-VCSEL that employed a hexagonal pattern of holes was also studied experimentally [6]. Its far-field pattern exhibited a minimum along the optical axis at relatively low bias currents. Two supermodes of a simplified 2×1 PC-VCSELs were compared on the basis of coupled-mode theory to explain this behavior.

II. Structure and theory

We simulated a similar RDPC-VCSEL to the one studied experimentally [6]. It was designed for 850 nm emission, and consisted of 20.5 pairs of top DBR with alternating p-type $\mathrm{Al_{0.12}Ga_{0.88}As/Al_{0.9}Ga_{0.1}As}$ layers, a λ-cavity with three quantum wells (QWs) at antinode position, and 34.5 pairs of n-type bottom DBRs. For the sake of simplicity, a uniform dopant concentration profile of 10^{18} $\mathrm{cm^{-3}}$ was assumed in both DBRs. An oxide aperture that provides the current confinement and has 25 $\mu\mathrm{m}$ diameter, was enclosed in the first high Al-content layer just above the cavity. A hexagonal PC pattern was etched into the top 16 pairs of DBR mirrors, which resulted in an etching-depth dependence factor of about 0.08 [1], close to the one in the measured laser. The lattice constant (Λ) of the PC was 5 $\mu\mathrm{m}$, and the diameters of the holes were set to 2.5 $\mu\mathrm{m}$. The diameter of the central one (d_0) was varied from 1.25 $\mu\mathrm{m}$ to 3.75 $\mu\mathrm{m}$, or remained unetched to serve as a simulation reference. The first ring of PC positions was left intact, forming the RD. A nonzero imaginary part of the refractive index of the QW material was selected to compensate for the optical loss of the fundamental mode of the reference 7-defect PC-VCSEL.

The optical modes of the RDPC-VCSEL were calculated by solving the 3-D scalar Helmholtz eigenvalue equation in a fully numerical fashion [7]. A triangular mesh was generated first that matched all transverse contours present in the RDPC-VCSEL, and was thereafter extruded to the 3-D structure. In order to decrease the computer demands, only a 30-degree section of the device was meshed two calculate non-degenerate modes, which exhibited perfect symmetry against 60-degree rotation. A 90-degree section was calculated for other, doubly degenerated modes. The transverse cross sections of the first few modes at the middle QW are shown on Fig. 1. The simulation of degenerated modes required about 20 GB memory, and took about 15 hours per mode on 2.4-GHz Opteron processor.

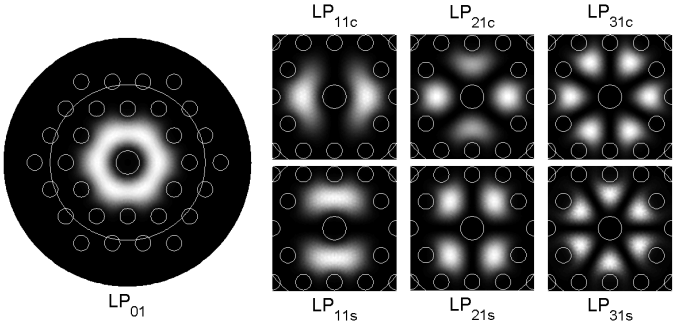

Fig. 1. Transverse cross sections of few lowest order modes of a RDPC-VCSEL, in which $d_0/\Lambda = 0.75$. The fundamental mode is shown in the whole computational window, higher order modes only in the central area. $\mathrm{LP_{11}}$ and $\mathrm{LP_{21}}$ modes are doubly degenerated if holes are etched in a hexagonal pattern. White curves indicate the etched holes and the oxide aperture.

978-1-61284-878-5/11/$26.00 ©2011 IEEE

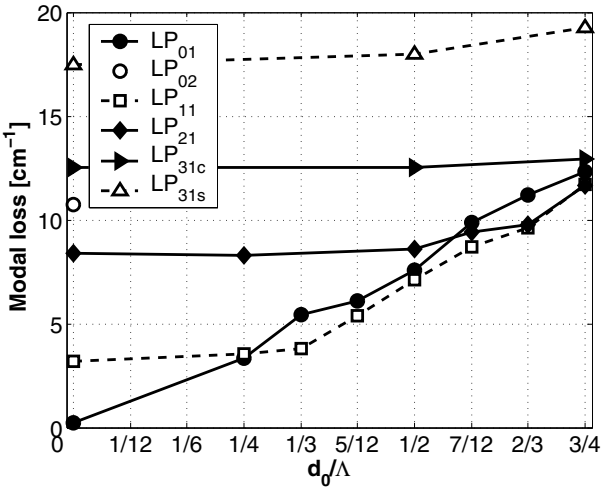

Fig. 2. Calculated modal losses of few lowest order optical modes of a RDPC-VCSEL. The LP_{02} mode of the 7-defect PC-VCSEL has a narrow, intense peak at the center, and a ring-shaped lobe still within the defect area.

III. Results

The left part of Fig. 2 shows that higher order modes of the 7-defect PC-VCSEL ($d_0/\Lambda = 0$) exhibited consequently increasing losses, because their lobes were squeezed outside, overlapped more with the etched holes, and thus suffered from larger scattering losses. Etching a central hole may alter their loss sequence, because higher azimuthal order modes tend to have less overlap with the central hole. As a consequence, it is expected that the central lobe had opposite effect on the modal losses. This is confirmed visually on Fig. 3, as more light leaves the cavity through the central hole from the fundamental mode than from modes having zero field along the optical axis.

It can be seen on Fig. 2 that the loss of the fundamental LP_{01} mode exceeded that of LP_{11} if $d_0/\Lambda > 0.25$. However, LP_{21} mode has even smaller loss for $d_0/\Lambda = 0.75$, although the difference from LP_{11} is marginal. Since all modes exhibit a distorted ring-like intensity distribution within the RD (note that the doubly degenerated modes should coexist, and their intensities could be summarized), their overlap with the gain region should be similar. Therefore one can expect that the mode with smallest optical loss starts lasing first, unless the current distribution is unrealistically inhomogeneous within the area of the RD. Our analysis explains correctly why an out-of-phase supermode was observed at relatively low bias current in the experiment [6].

The wavelengths of all modes are also naturally obtained from the real parts of eigenvalues from this analysis. There is no need for the rough approximation of substituting the RDPC-VCSEL with a coupled 2×1 PC-VCSEL array to explain the wavelength difference between the two supermodes, as was done in [6].

IV. Conclusion

A direct 3-D numerical solution of the scalar Helmholtz equation was applied successfully for the simulation of a RDPC-VCSEL. It has confirmed the observed higher-order mode emission from a similar device that had a central hole diameter of $d_0/\Lambda = 0.5$; without the need for the rough comparison with a coupled 2×1 PC-VCSEL array. It has been also shown that even higher order modes could start lasing first if the diameter of the central hole is larger.

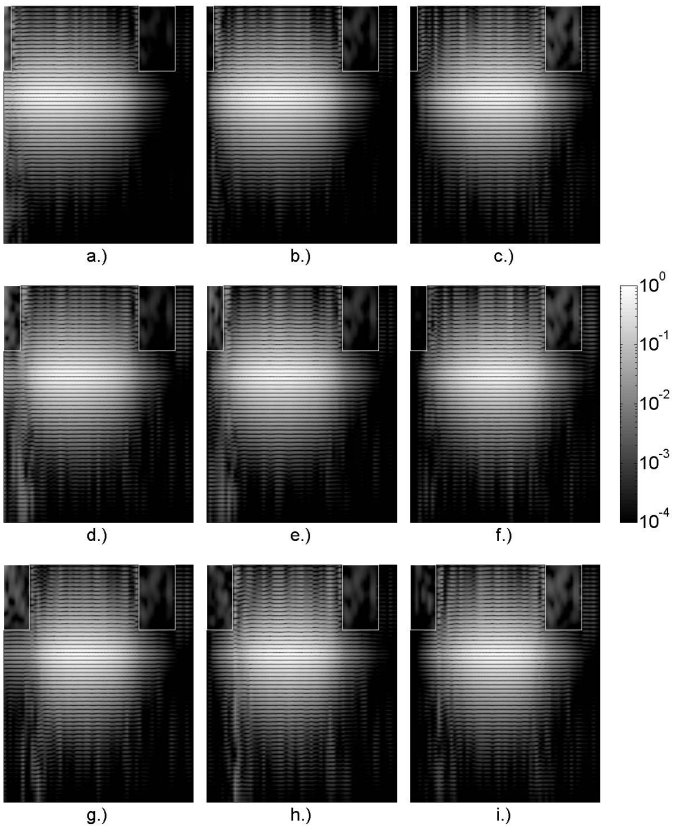

Fig. 3. Half axial cross sections of LP_{01} (a, d, g), LP_{11c} (b, e, h) and LP_{21c} (c, f, i) modes for $d_0/\Lambda = 0.25$ (a-c), 0.5 (d-f) and 0.75 (g-i), respectively. Higher order modes have zero intensity along the optical axis. White lines indicate the central hole and the one in 2Λ distance. The displayed sections are cut at the oxide radius, because the intensity is negligible outwards.

References

[1] N. Yokouchi, A. J. Danner, K. D. Choquette, "Two-dimensional photonic crystal confined vertical-cavity surface-emitting lasers," *IEEE J. Sel. Top. Quantum Electron.*, vol. 9, pp. 1439–1445, September/October 2003.

[2] R. A. Morgan, et al., "High-power coherently coupled 8×8 vertical cavity surface emitting laser array," *Appl. Phys. Lett.*, vol. 61., pp. 1160–1162, September 1992.

[3] J. J. Raftery Jr. et al., "In-phase evanescent coupling of two-dimensional arrays of defect cavities in photonic crystal vertical cavity surface emitting lasers," *Appl. Phys. Lett.*, vol. 89, 081119, August 2006.

[4] D. F. Siriani et al., "Mode control in photonic crystal vertical-cavity surface-emitting lasers and coherent arrays," *IEEE J. Sel. Top. Quantum Electron.*, vol. 15, pp. 909–916, May/June 2009.

[5] P. Nyakas, "Optical simulation of coupled defect cavities in photonic crystal vertical-cavity surface-emitting lasers," *Proc. SPIE*, 7720, 77201M, 2010.

[6] A. Liu et al., "Phase-locked ring-defect photonic crystal vertical-cavity surface-emitting laser," *Appl. Phys. Lett.*, vol. 96, 151103, April 2010.

[7] P. Nyakas et al., "Self-consistent real three-dimensional simulation of vertical-cavity surface-emitting lasers," *J. Opt. Soc. Am. B*, vol. 23, pp. 1761–1769, September 2006.